Journal of Organometallic Chemistry, 186 (1980) 213—236

THE MÖSSBAUER RECOIL-FREE FRACTION AND STRUCTURE

II *. DI-μ_3-OXO-BIS-(μ-DICHLORO)-BIS[μ-DIMETHYLTIN(IV)]-BIS-[CHLORODIMETHYLTIN(IV)], AND ITS ETHYL HOMOLOGUE

PHILIP G. HARRISON *, M.J. BEGLEY and K.C. MOLLOY

Department of Chemistry, University of Nottingham, University Park, Nottingham, NG7 2RD (Great Britain)

(Received August 3rd, 1979)

Summary

The crystal structure of the title compound, $[ClMe_2SnOSnMe_2Cl]_2$, the partial structure of its ethyl homologue, $[ClEt_2SnOSnEt_2Cl]_2$, and tin-119 Mössbauer data for the two compounds in the temperature range 77—175.5 K are reported. Crystals of $[ClMe_2SnOSnMe_2Cl]_2$ are monoclinic, space group $P2_1/c$, with a 7.258(1), b 18.581(6), c 8.733(8) Å, β 109.76(4)°, $Z = 4$.

The structure consists of centrosymmetric dimeric units held in a two-dimensional polymeric lattice by anionic chloride bridges. The central part of the dimeric unit consists of an essentially planar four-membered $Me_2SnOSnMe_2O$ ring, to the oxygen atoms of which are appended $[ClMe_2Sn]$ units. The geometries at both endo- and exo-cyclic tin atoms are similar, forming contacts to six neighbouring atoms in a distorted arrangement midway between trigonal bipyramidal and octahedral. Crystals of $[ClEt_2SnOSnEt_2Cl]_2$ are also monoclinic, space group $P2_1/n$, with a 10.3712(4), b 9.4699(6), c 15.9432(1) Å, β 106.43(3)°, $Z = 4$, but the structure has only been partly solved due to disorder. The major component of the disorder (~75%) has a structure similar to that of $[ClMe_2SnOSnMe_2Cl]_2$. The second component is best described as a series of alternating $[R_4Sn_2O_2]$ and $[R_2SnX_2]$ units, in which two of the latter units chelate $[Sn_2O_2]$ four-membered rings. Tin-119 Mössbauer isomer shift, quadrupole splitting, and recoil-free fraction temperature dependence have also been studied and correlated with the crystallographic data. The variation of the recoil-free fraction of $[Me_4Sn_2Cl_2O]_2$ varies linearly with temperature in the range 77—175.5 K with a temperature coefficient of -1.26×10^{-2} K^{-1}. In contrast, the ethyl compound exhibits a discontinuity at ca. 110 K, attributed to a phase change involving a relaxation of the coordination about one of the two crystallographically independent tin atoms.

---

* For part I see ref. 26.

Introduction

The structure adopted by compounds of the stoichiometry $R_4Sn_2X_2O$, commonly referred to as tetraorganostannoxanes, has been the subject of many reports since their discovery in 1914. Although initially thought to be monomeric [1], subsequent work [2] has conclusively demonstrated not only the presence of nonequivalent tin atoms in these compounds, but also their dimeric nature. Accordingly, structures I and II were proposed [2]. Of the available

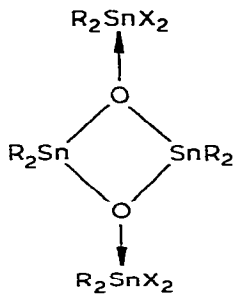

(I)

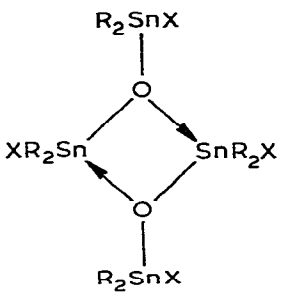

(II)

structural information on this type of compound, four reports are concerned with carboxylate derivatives (X = RCO_2—) whilst none deal with the simple halogeno compounds. The structures of $[Me_4Sn_2(OSiMe_3)_2O]_2$ [3] and $[Me_4Sn_2(NCS)_2O]_2$ [4] both adopt the so-called ladder structure III.

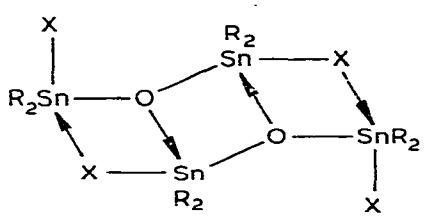

(III)

In both cases, planar $\overline{SnOSnO}$ rings are formed. While the structure of $[Me_4Sn_2(OSiMe_3)_2O]_2$ is more accurately described as a "staircase" since the exocyclic groups bend away from the plane of the Sn_2O_2 ring, the structure of $[Me_4Sn_2(NCS)_2O]_2$ is entirely co-planar. Similarly, while the two tin atoms in the trimethylsiloxy-derivative are both five-coordinated, the two tin atoms in the isothiocyanate derivative have differing coordination numbers. Thus, while the endocyclic tin atom is five coordinated, the exocyclic tin adopts a distorted octahedral six-coordinate geometry by virtue of a weak (3.33(3) Å) intermolecular Sn···S bond, resulting in a polymeric structure. Of the four carboxylate derivatives studied, the report on $Me_4Sn_2(OCOMe)_2O$ is very brief [5]. A partial structure of $[(CH_2{=}CH)_4Sn_2(OCOCF_3)_2O]_2$ has been reported [6], although the positions of the atoms in the CF_3 and vinyl groups could not be located. The geometry at each tin is best described as a distorted trigonal bipyramidal, but with a sixth oxygen atom weakly [Sn(endocyclic)···O = 2.66(5) Å] or very weakly [Sn(exocyclic)···O = 3.12(5) Å] coordinated. The structures of [(n-Bu_2-

$SnO_2CCl_3)_2O]_2$ [7] and $[(Me_2Sn(O_2CCF_3)_2O]_2$ [8] are virtually identical. One of the carboxylate groups is unidentate with one oxygen atom bridging two tins, whilst the other bridges two tin atoms using both oxygen atoms. Thus, one tin atom has distorted trigonal bipyramidal coordination, and the other has distorted six-coordinated environment.

In this paper we describe the structure of the chloroderivative $[Me_4Sn_2ClO_2O]_2$, and a partial structure of its ethyl homologue. In addition, the results of a tin-119 Mössbauer recoil-free fraction study are presented.

Experimental

A. The structure of $[Me_4Sn_2Cl_2O]_2$

(i) Crystal preparation. Equimolar quantities of dimethyltin dichloride and 2-amino-benzthiazole in the minimum quantity of acetone were stirred at room temperature for 24 h. The resulting pale orange solution was concentrated to approximately half its volume and the white precipitate which had formed removed by filtration. Crystals of the title compound were obtained from the filtrate after standing at room temperature for several days.

(ii) Crystal data. $C_4H_{12}Cl_2OSn_2$; M = 384.44, *a* 7.258(1), *b* 18.581(6), *c* 8.733(8) Å, β 109.76(4)°, *U* 1108.5 Å^3; *Z* = 4, *F*(000) = 712; Mo-K_α radiation, λ = 0.71069 Å; μ(Mo-K_α) = 49.42 cm^{-1}; Space Group = $P2_1/c$ from systematic absences (*h*0*l* for $l = 2n + 1$ and 0*k*0 for $k = 2n + 1$).

The space group and initial cell parameters were determined from oscillation and zero- and first-layer Weissenberg photographs. Relative intensities were collected up to $\theta = 25°$ with Mo-K_α radiation using a Hilger and Watts Y290 four-circle automatic diffractometer. Accurate cell dimensions were obtained by least-squares refinement of ca. 17 reflections. All reflections with $I < 3\sigma(I)$ were considered non-observed, reducing the total number of reflections from 1737 to 1648. The intensities were corrected for Lorentz and polarisation effects, no absorption correction was made due to the low μ value.

The asymmetric unit of the title compound consists of half the dimeric unit, the remainder of the atomic positions being symmetry generated.

The position of the two tin atoms in the asymmetric unit were determined by a three-dimensional Patterson synthesis, and the coordinates thus obtained used to phase the initial structure factor calculation. A Fourier synthesis at this stage yielded the positional parameters of the two chlorine atoms, and these along with the positional parameters of the two tin atoms were further refined by two cycles of full matrix least-squares isotropic refinement. Two further cycles of mixed (the tin atoms being varied anisotropically) least-squares refinement were required before a subsequent Fourier synthesis yielded the positions of the outstanding non-hydrogen light atoms. Two cycles of mixed and four cycles of full matrix anisotropic (all atoms) least-squares refinement produced a convergence of the "*R*" value at 0.091.

At this stage, the weighting scheme:

$$w = 1 \quad \text{for} \quad F_{obs} < P(1)$$

$$w = \frac{P(1)}{F_{obs}} \quad \text{for} \quad F_{obs} > P(1), \quad P(1) = 27.0$$

TABLE 1

FINAL FRACTIONAL ATOMIC COORDINATES IN $[Cl)CH_3)_2SnOSn(CH_3)Cl]_2$

Atom	x/a	y/b	z/c
Sn(1)	0.0626(2)	0.1629(9)	0.1587(1)
Sn(2)	0.0135(1)	0.4632(5)	0.3316(8)
Cl(1)	0.035(1)	0.112(3)	0.407(5)
Ci(2)	0.096(1)	0.320(2)	0.352(4)
O(1)	0.027(2)	0.062(5)	0.064(1)
C(1)	0.731(3)	0.445(1)	0.168(2)
C(2)	0.296(2)	0.481(1)	0.311(2)
C(3)	0.351(3)	0.189(1)	0.248(3)
C(4)	0.784(3)	0.212(1)	0.059(2)

Estimated standard deviations in parentheses.

was applied, and a subsequent four cycles of full matrix anisotropic least-squares refinement yielded a final "R" value of 0.087.

All calculations were performed using the CRYSTALS suite of programs [9]. Scattering factors for neutral atoms and the chloride anion were used [10].

Final fractional atomic coordinates and anisotropic thermal parameters are given in Tables 1 and 2 respectively. Tables 3 and 4 list the intra- and intermo-

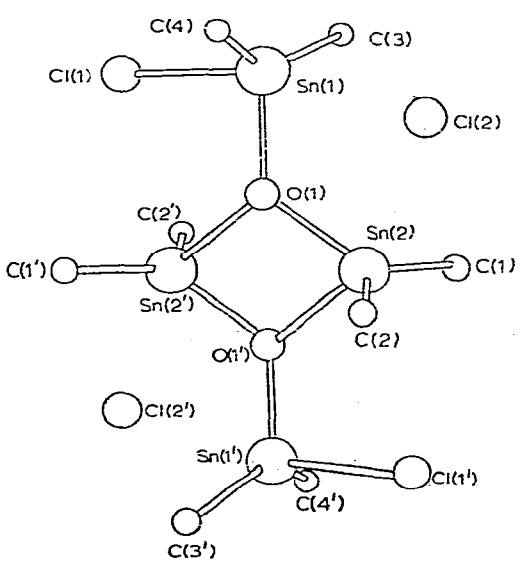

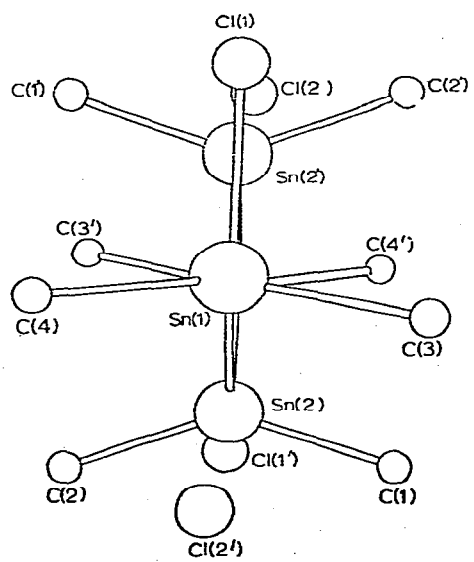

Fig. 1. The structure of $[ClMe_2SnOSnMe_2Cl]_2$ showing the atomic numbering (symmetry related atoms are primed).

Fig. 2. View of the molecular unit of $[ClMe_2SnOSnMe_2Cl]_2$ along the Sn(1)—O(1) bond showing the planar skeleton.

TABLE 2

FINAL ANISOTROPIC THERMAL PARAMETERS IN $[Cl(CH_3)_2SnOSn(CH_3)_2Cl]_2$

Atom	U_{11}	U_{22}	U_{33}	U_{23}	U_{13}	U_{12}
Sn(1)	7.61(8)	6.05(7)	4.07(6)	−0.52(4)	2.32(5)	−0.24(5)
Sn(2)	6.99(7)	6.93(7)	2.46(8)	−0.52(3)	2.28(4)	0.08(4)
Cl(1)	14.3(4)	10.0(3)	4.0(2)	0.4(2)	4.3(2)	−0.7(3)
Cl(2)	15.7(5)	6.9(3)	5.4(2)	−0.7(2)	5.1(3)	1.6(3)
O(1)	8.2(6)	5.2(5)	2.7(4)	−0.6(3)	2.5(4)	−0.6(4)
C(1)	7.0(10)	12.0(10)	4.4(9)	−1.1(9)	1.2(7)	−1.0(10)
C(2)	6.0(9)	10.0(10)	5.9(9)	0.1(9)	1.9(7)	−0.8(8)
C(3)	6.0(10)	12.0(20)	9.0(10)	−2.0(10)	3.0(9)	−2.0(10)
C(4)	7.0(10)	10.0(10)	8.0(10)	1.0(10)	3.0(9)	1.0(10)

Estimated standard deviations in parentheses. U_{ij} are of the form: $10^2 \exp -2\pi^2(h^2U_{11}a^{*2} + k^2U_{22}b^{*2} + l^2U_{33}c^{*2} + 2hkU_{12}a^*b^* + 2klU_{23}b^*c^* + 2hlU_{13}a^*c^*)$

lecular bond distances and angles; least-squares mean planes data is given in Table 5.

The molecular geometry of the title compound, with atomic labelling, is shown in Figs. 1 and 2, and a projection of the unit cell onto the *bc* plane in Fig. 3.

TABLE 3

INTRAMOLECULAR BOND DISTANCES (Å) AND ANGLES (°) IN $[Cl(CH_3)_2SnOSn(CH_3)_2Cl]_2$

(a) Bond distances			
Sn(1)—Cl(1)	2.438(4)	Sn(2)—Cl(2)	2.710(5)
Sn(1)—Cl(2)	2.788(5)	Sn(2)—O(1)	2.054(8)
Sn(1)—C(1)	2.029(9)	Sn(2)—O(1′)	2.115(9)
Sn(1)—C(3)	2.090(20)	Sn(2)—C(1)	2.090(20)
Sn(1)—C(4)	2.120(20)	Sn(2)—C(2)	2.140(20)
		Sn(2)—Cl(1′)	3.411(5)
(b) Bond angles			
Cl(1)—Sn(1)—C(3)	98.3(6)	C(1)—Sn(2)—C(2)	135.3(7)
Cl(1)—Sn(1)—C(4)	100.2(5)	C(1)—Sn(2)—O(1)	110.4(6)
Cl(1)—Sn(1)—Cl(2)	163.5(2)	C(1)—Sn(2)—O(1′)	100.6(6)
Cl(1)—Sn(1)—O(1)	88.1(3)	C(1)—Sn(2)—Cl(2)	92.0(6)
C(3)—Sn(1)—C(4)	140.6(9)	C(1)—Sn(2)—Cl(1′)	80.5(6)
C(3)—Sn(1)—Cl(2)	85.3(6)	C(2)—Sn(2)—O(1)	113.0(6)
C(3)—Sn(1)—O(1)	110.0(7)	C(2)—Sn(2)—O(1′)	100.5(6)
C(4)—Sn(1)—Cl(2)	85.5(5)	C(2)—Sn(2)—Cl(2)	87.5(6)
C(4)—Sn(1)—O(1)	105.2(7)	C(2)—Sn(2)—Cl(1′)	74.3(5)
Cl(2)—Sn(1)—O(1)	75.6(3)	O(1)—Sn(2)—O(1′)	74.9(4)
		O(1)—Sn(2)—Cl(2)	77.1(3)
Sn(2)—O(1)—Sn(2′)	105.1(4)	O(1)—Sn(2)—Cl(1′)	138.7(3)
Sn(2)—O(1)—Sn(1)	124.4(4)	O(1)—Sn(2)—Cl(2)	151.8(2)
Sn(2′)—O(1)—Sn(1)	130.1(4)	O(1′)—Sn(2)—Cl(1′)	63.8(2)
		Cl(2)—Sn(2)—Cl(1′)	143.9(1)
Sn(1)—Cl(2)—Sn(1)	82.3(1)		
Sn(1)—Cl(1)—Sn(2′)	78.0(6)		

Symmetry related atoms are primed.
Estimated standard deviations in parentheses.

TABLE 4

INTERMOLECULAR BOND DISTANCES (Å) AND ANGLES (°) IN $[Cl(CH_3)_2SnOSn(CH_3)_2Cl]_2$

(a) Distances	
Sn(1)—Cl(2″)	3.348(5)
(b) Angles	
Cl(2″)—Sn(1)—O(1)	172.2(3)
Cl(2″)—Sn(1)—Cl(1)	84.5(2)
Cl(2″)—Sn(1)—Cl(2)	111.88(8)
Cl(2″)—Sn(1)—C(3)	73.5(6)
Cl(2″)—Sn(1)—C(4)	74.0(6)
Sn(1)—Cl(2)—Sn(1″)	124.5(2)
Sn(2)—Cl(2)—Sn(1″)	147.7(2)

Atoms from a second dimeric unit are double primed
Estimated standard deviation in parentheses

TABLE 5

THE EQUATIONS OF LEAST SQUARES PLANES, DEVIATIONS (Å) OF ATOMS FROM THE PLANES, AND ANGLES BETWEEN THE PLANES (°) IN $[ClMe_2SnOSnMe_2Cl]_2$

Plane 1:	Sn(2), Sn(2′), O(1), O(1′)
	$7.04214x + 0.62203y - 0.89452z = -0.068$
	Sn(2), 0.155; Sn(2′), −0.018; O(1), 0.028; O(1′), −0.164.
Plane 2:	Sn(2), C(1), C(2)
	$1.11791x - 10.90141y + 6.07998z = -3.018$
	Sn(2), 0.00; C(1), 0.00; C(2), 0.00
Plane 3:	Sn(2), O(1), Sn(2′), Sn(1), Cl(1)
	$7.04263x + 0.48743y - 0.88955z = -0.021$
	Sn(1), 0.040; Sn(2), 0.047; Sn(2′), −0.005; O(1), −0.075; Cl(1), −0.007; Cl(2), 0.540.
	Sn(1), C(3), C(4), Cl(1)
	$0.96919x - 17.49349y - 2.93912z = -3.301$
	Sn(1), 0.045; C(3), 0.393; C(4), 0.170; Cl(1), 0.177
	Angles between planes 1 and 2 = 71.31°
	Angles between planes 3 and 4 = 88.25°

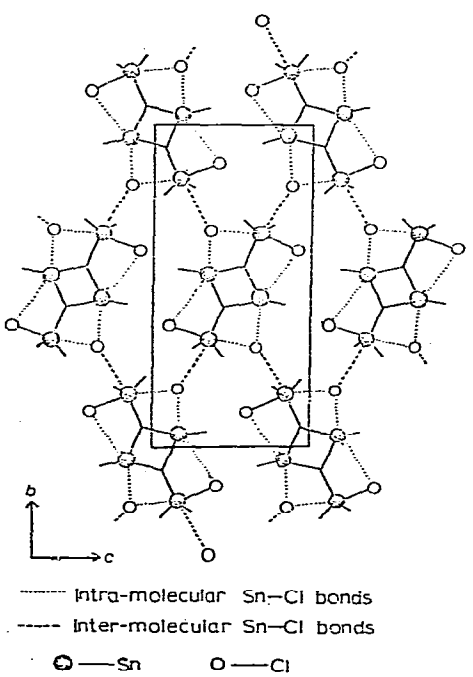

Fig. 3. Projection of the unit cell of $[ClMe_2SnOSnMe_2Cl]_2$ onto the *bc* plane.

B. The structure of $[Et_4Sn_2Cl_2O]_2$

(i) Crystal preparation. Crystals of the title compound were prepared by the method of Johnson [11]; slow evaporation of an acetone solution yielded crystals of a nature suitable for intensity measurements. A crystal of approximate dimensions 0.3 × 0.25 × 0.1 mm, stable to both air and X-rays, was mounted on a glass fibre and used for initial cell measurements and subsequent intensity data collection.

(ii) Crystal data. $C_8H_{20}Cl_2OSn_2$; M = 440.56; a 10.3712(4), b 9.4699(6), c 15.9432(1) Å, β 106.43(3)°; U 1502.12 Å^3, Z = 4; $F(000)$ = 880; Mo-K_α radiation, λ 0.71069 Å; μ(Mo-K_α) 36.61 cm^{-1}. Space group $P2_1/n$ by systematic absence ($0k0$ for $k = 2n + 1$ and $h0l$ for $h + l = 2n + 1$).

Using the same procedure as before, relative intensities were collected up to θ = 25.0° yielding 1475 usable reflections. The intensities corrected for Lorentz and polarisation effects, no absorption correction being required due to the low μ value.

The positional parameters of the two tin atoms were obtained by Patterson methods and used to phase the initial structure factor calculation. After one cycle of full matrix isotropic least-squares refinement of these parameters, a Fourier synthesis yielded the positions of two chlorine atoms, one oxygen and one carbon atom which fitted a chemically acceptable model. However, in the course of a further eight cycles of isotropic refinement, all but one of these atoms, a chlorine, was rejected on the basis of unacceptable thermal parameters. The remaining three atoms were thus refined by two cycles of mixed (the tins varying anisotropically) refinement, and a subsequent Fourier synthesis yield the positional parameters of two chlorine and two oxygen atoms. Although chemically acceptable the low "weights" of the peaks assigned to chlorine atoms suggested a degree of disorder in the structure, and thus the occupancies of these and the two oxygens were limited to 0.5. Following two cycles of mixed refinement, Fourier synthesis yielded the positions of four light atoms, assigned on a chemical basis as carbon atoms, although all of these were rejected after two further cycles of mixed refinement, by inspection of their thermal parameters.

In addition to the tin atoms, the whole occupancy chlorine was now allowed to vary anisotropically; the occupancies of the remaining chlorine atoms were also allowed to vary. After two cycles of mixed refinement, the positions of six (carbon) atoms were located by Fourier methods, but again, were subsequently rejected after two further cycles of mixed refinement.

The thermal parameters of all the atoms thus far located with any certainty were now sufficiently stable to allow them all to vary anisotropically, and after two cycles of full matrix least-squares anisotropic refinement and a Fourier synthesis, possible positional parameters for seven carbon atoms were obtained. Of these, four were bonded directly Sn(1), and one to Sn(2). Allowing for disorder at the α-carbon of the ethyl groups at Sn(1), the occupancies of the four carbons bonded to Sn(1) were limited to 0.5, whilst the remaining three carbon atoms were assigned occupancies of 1.0. In addition, refinement of the occupancies of the two "low weight" chlorine atoms had stabilised the occupancy of the chlorine bonded to Sn(1) at 1.1 and that of the chlorine bonded to Sn(2) at 0.3.

The chlorine at Sn(2) was thus reassigned to a carbon of occupancy 1.0, and the occupancy of the chlorine bonded to Sn(1) fixed at 1.0.

After two cycles of mixed refinement, one of the carbons bonded to Sn(2) was rejected on the basis of its thermal parameters. The position of the other carbon (formerly a chlorine) was, however, unacceptable chemically as such, and was reassigned to a chlorine of occupancy 0.3, the occupancy of the chlorine attached to Sn(1) being altered to 0.7.

In an attempt to account more fully for the disordered alkyl groups (at Sn(1)) the occupancies of the α-carbons were allowed to vary, although this merely produced chemically unacceptable atoms after two cycles of mixed refinement. The six carbons were thus rejected, but were relocated and reassigned (occupancies 0.5 and 2.0 for α- and β-carbons respectively) after two further cycles of mixed refinement followed by a Fourier synthesis. To account for the presence of a persistent area of electron density at ca. 2.7 Å from Sn(1) but very close (ca. 0.6 Å) to the chlorine found in the initial Fourier synthesis, the highest weight peak in the latest Fourier synthesis was assigned a chlorine atom of occupancy 0.3.

During the course of six subsequent cycles of refinement, two mixed, two with all known atoms varying anisotropically, Fourier syntheses failed to yield the position of carbon atoms either α or β to Sn(2), which remained chemically acceptable on further refinement.

The disorder in the oxygen and chlorine atoms was normalised (to 0.75 and 0.25) throughout the molecule, maintaining the occupancies of the α- and β carbons at Sn(1) at 0.5 and 1.0 respectively. Such changes could not be accommodated directly by anisotropic refinement, so the thermal parameters of all atoms were returned to their last isotropic temperature parameter. Four cycles of isotropic least-squares refinement and two cycles of mixed refinement in which the two tin atoms were allowed to vary anisotropically, produced a conventional "R" value of 0.177.

All calculations were performed using the CRYSTALS suite of programs [9]. Scattering factors used were those for neutral atoms [10].

TABLE 6

FINAL FRACTIONAL ATOMIC COORDINATES IN $[ClEt_2SnOSnEt_2Cl]_2$

Atom	x/a	y/b	z/c
Sn(1)	0.1376(4)	0.1090(5)	0.0672(3)
Sn(2)	0.4898(8)	0.0999(9)	0.0646(5)
O(1)	0.272(7)	0.042(8)	0.027(5)
O(2)	0.939(9)	0.042(10)	0.021(6)
Cl(1)	0.041(3)	0.254(4)	0.166(2)
Cl(2)	0.649(5)	0.110(6)	0.057(3)
Cl(3)	0.412(5)	0.283(5)	0.170(3)
Cl(4)	0.769(2)	0.100(3)	0.076(2)
C(1)	0.178(10)	0.010(11)	0.185(6)
C(2)	0.260(10)	0.476(11)	0.336(7)
C(3)	0.312(11)	0.069(12)	0.246(7)
C(4)	0.104(19)	0.331(20)	0.007(12)
C(5)	0.651(12)	0.228(13)	0.474(7)
C(6)	0.542(9)	0.198(10)	0.429(6)

Estimated standard deviations in parentheses

TABLE 7

FINAL ANISOTROPIC (U_{ij}) [a] AND ISOTROPIC (U[ISO]) [b] THERMAL PARAMETERS AND OCCUPANCIES IN $[ClEt_2SnOSnEt_2Cl]_2$

Atom	OCC	U[ISO]	U_{11}	U_{22}	U_{33}	U_{23}	U_{13}	U_{12}
Sn(1)	1.00		5.0(2)	5.1(2)	6.3(2)	0.6(3)	1.7(2)	−0.2(3)
Sn(2)	1.00		11.1(6)	13.0(5)	16.1(5)	0.9(5)	2.7(5)	−1.2(5)
O(1)	0.75	12.1(23)						
O(2)	0.25	1.1(26)						
Cl(1)	0.75	11.0(10)						
Cl(2)	0.25	4.3(11)						
Cl(3)	0.25	4.6(12)						
Cl(4)	0.75	3.2(8)						
C(1)	0.50	4.7(24)						
C(2)	0.50	5.5(25)						
C(3)	1.00	19.7(40)						
C(4)	0.50	10.3(50)						
C(5)	0.50	4.6(30)						
C(6)	1.00	11.9(28)						

[a] U_{ij} are of the form: $10^2 \exp -2\pi^2(h^2U_{11}a^{*2} + k^2U_{22}b^{*2} + l^2U_{33}c^{*2} + 2hkU_{12}a^*b^* + 2klU_{23}b^*c^* + 2hlU_{13}a^*c^*)$. [b] U[ISO] values have been multiplied by 10^2. Estimated standard deviations in parentheses.

TABLE 8

FINAL INTER- AND INTRAMOLECULAR BOND DISTANCES (Å) AND ANGLES (°) IN THE DISORDERED STRUCTURE OF $[ClEt_2SnOSnEt_2Cl]_2$ [a]

Structure A			
(1) Distances			
Sn(1)—Cl(1)	2.51(3)	Sn(2)—O(1)	2.24(17)
Sn(1)—Cl(2)	3.37(1)	Sn(2)—O(1′)	3.48(20)
Sn(1)—O(1)	1.80(20)	Sn(2)—Cl(2′)	2.84(1)
Sn(1)—C(1)	2.03(9)		
Sn(1)—C(2)	2.05(10)	Sn(1″)—Cl(2)	3.87(2)
Sn(1)—C(4)	2.29(13)		
Sn(1)—C(5)	2.17(4)	C(1)—C(3)	1.62(23)
		C(2)—C(3)	1.60(16)
		C(4)—C(6)	1.27(21)
		C(5)—C(6)	1.19(12)
(2) Angles			
Cl(1)—Sn(1)—Cl(2)	174(2)	Cl(2′)—Sn(1)—C(1)	84(2)
Cl(1)—Sn(1)—Cl(2′)		Cl(2′)—Sn(1)—C(2)	105(4)
Cl(1)—Sn(1)—O(1)	154(2)	Cl(2′)—Sm(1)—C(4)	90(2)
Cl(1)—Sn(1)—C(1)	71(4)	Cl(2′)—Sn(1)—C(5)	107(3)
Cl(1)—Sn(1)—C(2)	94(2)	O(1)—Sn(1)—C(1)	100(3)
Cl(1)—Sn(1)—C(4)	73(5)	O(1)—Sn(1)—C(2)	76.3(3)
Cl(1)—Sn(1)—C(5)	98(2)	O(1)—Sn(1)—C(4)	103(4)
Cl(2)—Sn(1)—Cl(2′)	119(4)	O(1)—Sn(1)—C(5)	99(2)
Cl(2)—Sn(1)—O(1)	29(2)	C(1)—Sn(1)—C(2)	25(3)
Cl(2)—Sn(1)—C(1)	104(4)	C(1)—Sn(1)—C(4)	140(7)
Cl(2)—Sn(1)—C(2)	82(2)	C(1)—Sn(1)—C(5)	157(6)
Cl(2)—Sn(1)—C(4)	111(5)	C(2)—Sn(1)—C(4)	150(5)
Cl(2)—Sn(1)—C(5)	86(2)	C(2)—Sn(1)—C(5)	147(4)
Cl(2′)—Sn(1)—O(1)	151(2)	C(4)—Sn(1)—C(5)	25(5)
Sn(1)—O(1)—Sn(2)	130(3)	Sn(1)—C(1)—C(3)	108(10)
Sn(1)—O(1)—Sn(2′)	175(3)	Sn(1)—C(2)—C(3)	108(5)
Sn(2)—O(1)—Sn(2′)	55(4)	Sn(1)—C(4)—C(6)	101(10)
		Sn(1)—C(5)—C(6)	111(10)
O(1)—Sn(2)—O(1′)	125(4)		
O(1)—Sn(2)—Cl(2′)	162(4)		
O(1′)—Sn(2)—Cl(2′)	37(1)		
Sn(1)—Cl(2)—Sn(2′)	116(1)		
Sn(1)—Cl(2)—Sn(1′)	61(4)		
Sn(1′)—Cl(2)—Sn(2′)	174(1)		
Structure B [b]			
(1) Distances			
O(2′)—Sn(1)—O(2)	52(5)	Sn(1)—Cl(3)—Sn(2)	75(2)
O(2′)—Sn(1)—Cl(3)	163(3)		
O(2′)—Sn(1)—Cl(4)	95(3)	Sn(1)—Cl(4)—Sn(2)	67(1)
O(2)—Sn(1)—Cl(3)	145(3)	Sn(1)—Cl(4)—Sn(2″)	122(2)
O(2)—Sn(1)—Cl(4)	43(3)	Sn(2)—Cl(4)—Sn(2″)	55(1)
Cl(3)—Sn(1)—Cl(4)	102(2)		

[a] Estimated standard deviations in parentheses. Symmetry related atoms are primed; atoms from a second dimeric unit are double primed. [b] The Sn—C and C—C bond lengths, and C—Sn—C angles and the angles at the α-carbon are the same as for Structure A.

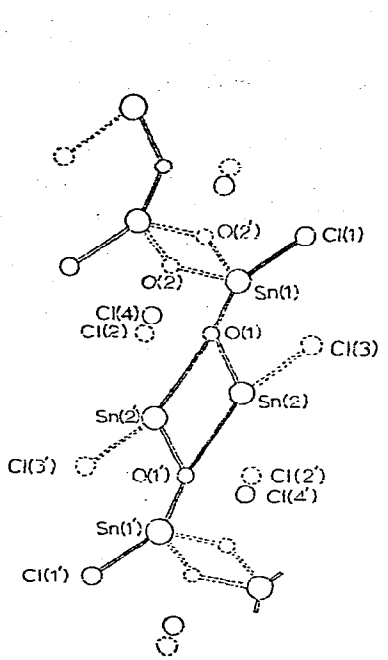

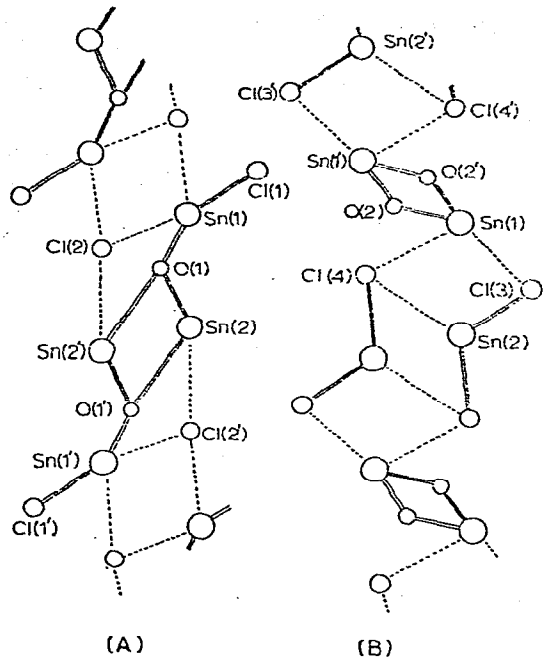

Fig. 4. The disordered structure of $[ClEt_2SnOSnEt_2Cl]_2$ (disordered ethyl groups omitted for clarity, symmetry related atoms are primed).

Fig. 5. Resolution of the disordered structure of $[ClEt_2SnOSnEt_2Cl]_2$ into the major (A) and minor (B) components (disordered ethyl groups are omitted for clarity.

Final fractional atomic coordinates are listed in Table 6, occupancies and the relevant thermal parameters (U[ISO] or U_{ij}) in Table 7, and intra- and intermolecular bond distances and angles in Table 8. The molecular geometry of the compound is shown in Figs. 4—6.

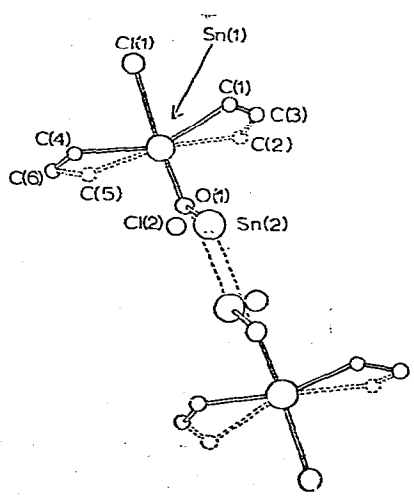

Fig. 6. The structure of $[ClEt_2SnOSnEt_2Cl]_2$ showing the atomic numbering of the disordered ethyl groups (structure A only).

C. Tin-119 Mössbauer studies

The spectrometer and data reduction procedures have been described previous [12].

Temperatures were varied using a Harwell CTC 200 Temperature Unit in conjunction with a thermocouple attached to the sample holder. At each temperature setting, the temperature was allowed to equilibrate for 2.5 hours or until such time that a steady temperature was reached. Temperatures were measured using a CROPICO Thermacouple Potentiometer (Croydon Precision Instrument Co.), accurate to ±1°C. Each spectrum was counted for at least 10^6 counts, although as the temperature increases spectrum quality decreases, requiring an increase in the counting time.

Raman data was obtained using a Spectra Physica 164 Argon$^+$ Laser.

Discussion

A. The structure of $[Me_4Sn_2Cl_2O]_2$

The structure of $[ClMe_2SnOSnMe_2Cl]_2$ consists of centrosymmetric dimeric units held in a two-dimensional polymeric lattice by anionic chloride bridges (Fig. 5). The central part of the dimeric unit consists of a four membered SnOSnO ring, which is essentially planar (Table 5), and maintains internal angles (74.9(4)°, 105.1(4)°) consistent with those noted for other distannoxane systems (105.0(20)°, $[Me_4Sn_2(NCS)_2O]_2$ [4], and 103.0(20)°, $[Vin_4Sn_2(O_2CCF_3)_2O]_2$ [6]. The three Sn—O bond distances (2.029(9), 2.054(8) and 2.115(9) Å) are very similar, reflecting the strong coordination within the dimer. These distances are, however, consistent with similar bond in other distannoxanes (Table 9), with the exception of $[Me_4Sn_2(OSiMe_3)_2O]_2$ [3] where the dimeric species is held together by a very weak Sn—O coordinate bond (2.80 Å).

Although generally similar in structure to the other distannoxanes reported [3—8], in particularly $[Me_4Sn_2(NCS)_2O]_2$ [4], $[Me_4Sn_2Cl_2O]_2$ maintains an essential difference in the disposition of its (pseudo)halide groups. One chlorine atom, (Cl(1)) is localised at Sn(1) by a covalent bond (2.438(4) Å) consistent with Sn—Cl bonds in other compounds (e.g. 2.32(2) Å in Ph_3SnCl [13] and

TABLE 9

A COMPARISON OF BOND LENGTHS (Å) AND ANGLES (°) IN $[Me_4Sn_2Cl_2O]_2$ WITH THOSE IN RELATED COMPOUNDS

Compound	Sn—O(b)	Sn—O(c)	O—Sn—O	Sn—O—Sn	Reference
$[ClMe_2SnOSnMe_2Cl]_2$	2.029(9) 2.054(8)	2.115(9)	74.9(4)	105.1(4)	This work
$[(SCN)Me_2SnOSnMe_2(NCS)]_2$	2.05(8) 1.99(3)	2.15(4)		105.0(20)	4
$[(CF_3CO_2)Vin_2SnOSnVin_2(O_2CF_3)]_2$	2.06(5) 2.11(5)	2.08(5)		103.0(20)	6
$[(Me_3SiO)Me_2SnOSnMe_2(OSiMe)_3)]_2$	2.20	2.80			3
$[(CF_3CO_2)Me_2SnOSnMe_2(O_2CCF_3)]_2$	2.039(5) 2.137(4)	2.040(4)	77.5(2)	102.5(2)	8

2.366(5), 2.365(6) Å in $Cl_2Sn[ON(Ph) \cdot CO \cdot Ph]_2$ [14], although it does exhibit a very weak intramolecular interaction with Sn(2) (3.411(5) Å) which may account for the slight lenghtening of this bond. Cl(2) on the other hand lies midway between Sn(1) (2.788(4) Å) and Sn(2) (2.710(5) Å) and is effectively a chloride anion. Its delocalisation may, in part, be attributed to its intermolecular bridging function, in which dimeric stannoxane units are linked by tin—chloride anion bridges (3.348(5) Å).

The geometries at the endo- and exo-cyclic tin atoms are essentially similar, both forming contacts to six neighbouring atoms, arranged in distorted geometry midway between octahedral and trigonal bipyramidal. The exocyclic tin, Sn(1), is coplanar with the plane of the stannoxane ring (Table 5, Fig. 3) and is surrounded by *trans*-carbon (C(3), C(4)) and *trans*-chlorines (Cl(1), Cl(2)) and by an oxygen (O(1)) and a chloride anion (from a second dimeric unit, Cl(2″)) which are also mutually *trans*. Distortions in the bond angles are, however, gross. The angles between mutually *trans*-groups are all closed from the ideal value of 180° to 163.5(2)° (Cl(1)—Sn(1)—Cl(2)), 172.2(3)° (O(1)—Sn(1)—Cl(2″)) and 140.6(9)° (C(3)—Sn(1)—C(4)).

The overall geometry at Sn(1) is best described as that of a *cis*-R_2SnXYZ trigonal-bipyramid, in which the presence of a long intermolecular interaction in the equatorial plane, bisecting the C(3)—Sn(1)—C(4) angle, increases the coordination at tin to 6, and opens the C—Sn—C angle from 120° to 140.6(9)°.

The geometry at Sn(2) can be described in a similar manner: that of a *cis*-R_2SnXYZ trigonal-bipyramid in which the presence of a long intramolecular interaction (Sn(2)—Cl(1′) 3.411(5) Å) increases coordination at Sn(2) to 6. Since the two oxygens and two chloriness are coplanar, the resulting geometry is *trans*-carbons, *cis*-chlorines, *cis*-oxygens in a distorted octahedron, although the angles at Sn(2) between *cis*-groups (O(1)—Sn(2)—O(1′) = 74.9(4)°, Cl(2)—Sn(1)—Cl(1′) = 143.9(1)°) are far from regular.

The Sn—C bonds to both tins (2.09(2), 2.12(2), 2.09(2) and 2.14(2) Å) are all consistent with the values observed in other methyltin derivatives e.g. 2.06(1) Å in Me_2SnF_2 [4,6] or the mean Sn—C distance in a variety of organotin compounds (2.18(3) Å) [16].

B. The structure of $[Et_4Sn_2Cl_2O]_2$ (partial determination)

The structure of $[ClEt_2SnOSnEt_2Cl]_2$ has been only partially determined and the high errors in the bond distances and angles precludes precise interpretation and comparison. The gross structure is, however, clear, and found to consist of two resolvable components which are highly disimilar (Fig. 5).

The major component of the disorder (75%), structure A, is similar to the structure of $[ClMe_2SnOSnMe_2Cl]_2$ discussed above. Planar, dimeric units, containing a four-membered SnOSnO ring are linked in a polymeric fasion by anionic chloride bridges. Two types of Sn—O bond are now observable, and distinct monomeric parts of the overall dimer can be distinguished. Within this monomeric fraction, the Sn—O distances (1.80(20) and 2.24(17) Å) are different, but, within experimental error, are comparable to those in the analogous methyl compound (2.029(9), 2.054(8) Å). The Sn—O coordinate bond, however, (3.48(20) Å) is now much longer than before (2.115(9) Å) and represents only a very weak interaction.

The disposition of the two chlorine atoms is also similar to those in the methyl analogue, although now their function is more complex. One chlorine is again localised at the exo-cyclic tin by a covalent bond (2.51(3) Å), but this no longer coordinates intramolecularly to the endo-cyclic tin. The role of the chloride anion is twofold: (1) to supplement the weak Sn—O coordinate bond in holding the dimeric unit together, by forming two intramolecular bridges 3.37(1), 2.84(1) Å cf. Sn···Cl = 3.54(5) Å in Me_2SnCl_2 (43)) and (2) linking individual dimeric units by a very weak bridging interaction (3.87(2) Å). This latter interaction results in the formation of planar ribbons of loosely bound distannoxane units (Fig. 5).

The geometry and coordination number at the two tins is different, Sn(1) can be described as a *trans*-R_2SnXYZ trigonal-bipyramid (C—Sn—C = 140(7)—157(6)°) depending on the disorder of the ethyl groups) in which a weak intermolecular interaction (Cl(2'')—Sn(1) = 3.87(2) Å) bisecting the Cl—Sn—Cl angle increases coordination at Sn(1) to 6 and opens the Cl(1)—Sn(1)—Cl(2) angle to 174(2)°.

Although no ethyl groups bonded to Sn(2) have been located, the presumed geometry at Sn(2) is that of a five-coordinate *trans*-R_2SnXYZ trigonal-bipyramidal by (a) analogy with the geometry at Sn(1) and (b) due to the visible planarity of the $[O_2SnCl]$ moiety. In both cases, large deviations from ideal geometry occur, the relevant angles being listed in Table 8.

In the minor component (25%) of the disorder (B, Fig. 5), loosely bound planar ribbons are again formed, but are held together in a very different manner to those in Structure A. SnOSnO ring formation now takes place between symmetry related tin atoms, Sn(1) and Sn(1'), and is very much tighter (2.08(11), 2.01(13) Å) than in Structure A (2.24(17), 3.48(20) Å). The other tin is very loosely bound, and is held to the stannoxane ring by a series of chlorine bridges. The very high primary anisotropic thermal parameters, U_{11}, U_{22} and U_{33} for Sn(2) (11.1(6), 13.0(6), 16.1(5) × 10^{-2}) compared to Sn(1) (5.0(2), 5.1(2), 6.3(2) × 10^{-2}) are no doubt a consequence of this minor component of the disorder.

One chlorine is again localised nearer the exo-cyclic tin (now Sn(2)), although the bond distance (2.67(8) Å) is long for a covalent Sn—Cl bond, an coordinate intramolecularly to Sn(1) (3.30(7) Å) in a similar manner to that observed in the analogous methyl compound. The long Sn(2)—Cl(3) bond is caused by the requirements of a relatively strong Sn(1)···Cl(3) bridge (cf. Sn···Cl = 3.54(5) Å in Me_2SnCl_2 [17]) to maintain a dimeric distannoxane unit. Further stabilisation of the position of Sn(2) comes from an anionic chloride, Cl(4), which bridges between Sn(1) (3.30(5) Å) and Sn(2) (3.33(7) Å). The formation of polymeric ribbons via intermolecular anionic chloride bridges (2.73(5) Å) also helps stabilise the position of Sn(2).

Structure B is perhaps best described as a series of alternating $[R_4Sn_2O_2]$ and $[R_2SnX_2]$ units in which two $[R_2SnX_2]$ moieties chelate $[Sn_2O_2]$ four-membered rings (cf. structure I). This is comparable to the chain structure adopted by diethyltin dichloride [18]. (Fig. 7), as are the Sn···Cl distances in the two compounds: Sn(1)—Cl(4): 3.30(7) Å, Sn(1)—Cl(3): 3.30(5) Å, Sn(2)—Cl(4): 3.33(7) Å in Structure B, Sn—Cl: 3.483(4), 3.440(4) Å in Et_2SnCl_2 [18].

The geometries at the two tins are the same as in Structure A i.e. six-coordi-

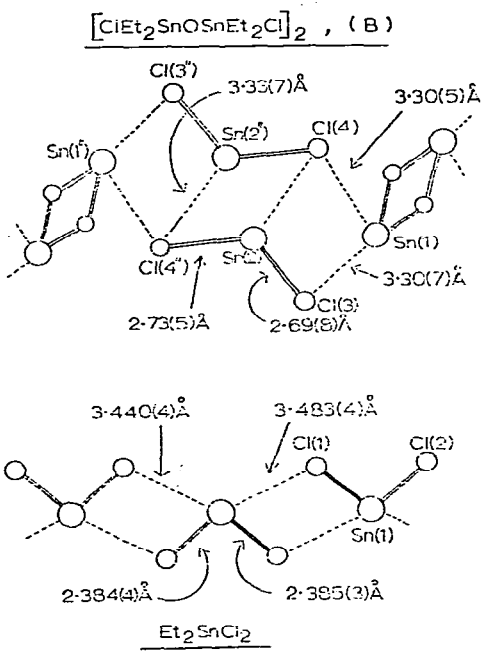

Fig. 7. Comparison of the structure of $[ClEt_2SnOSnEt_2Cl]_2$ (Structure B) and Et_2SnCl_2 showing the Sn—Cl bonding (ethyl groups omitted for clarity).

nate octahedral at Sn(1) and *trans*-R_2SnXYZ trigonal-bipyramidal at Sn(2), although the extent of the deviations from regularity is different, and angles around the tin atoms are given in Table 8.

Location of the ethyl groups, whose position seems independent of Structure A or B, is, at best uncertain, at worst unknown. The ethyl groups at Sn(1) have been localised and found to be disordered (50/50) at the α-carbon of the ethyl groups. The tin—carbon bonds (2.03(9)—2.29(13) Å) compare well with those in other compounds (2.18(3) Å (171)). The spread in the observed C—C bonds (1.19(12)—1.62(23) Å) and the high isotropic temperature factors for the β-carbons ($19.7(40) \times 10^{-2}$, C(3) and $11.9(25) \times 10^{-2}$, C(6) is probably due to a small amount of disorder at the β-carbons as a consequence of the disorder at the α-carbons. Location of the ethyl groups at Sn(2) has been unsuccessful and is indicative of further disorder.

C. Tin-119 Mössbauer studies

Tin-119 Mössbauer data for $[ClMe_2SnOSnMe_2Cl]_2$ and $[ClEt_2SnOSnEt_2Cl]_2$ at various temperatures in the range 77—175.5 K are listed in Tables 10 and 11 respectively. In both cases, the presence of a single quadrupole split resonance at all temperatures, indicating the equivalent of the environment of the two crystallography dissimilar tin nuclei in each, reflects the relative insensitivity of the I.S. and Q.S. to subtle changes in atomic environment. However, the resonance lines are quite broad and indicative of an envelope of overlapping peaks. Previous evidence for the non-equivalence of the two tin atoms in this type of compound comes from the observation of two broad resonances in the ^{119}Sn

(Continued on p. 230)

TABLE 10

TIN-119 MÖSSBAUER DATA FOR $[ClMe_2SnOSnMe_2Cl]_2$

Temp. (K)	I.S. [a]	Q.S. [a]	Γ_- [a, c]	Γ_+ [a, c]	A_- [b, c]	A_+ [b, c]	Total resonance area [b]	Relative %age effect
77	1.280	3.172	1.206	1.383	4.795	5.219	10.014	1.000
84	1.290	3.166	1.179	1.291	4.612	4.763	9.375	0.924
87.5	1.294	3.169	1.088	1.319	4.149	4.251	8.400	0.905
92	1.285	3.137	1.110	1.274	3.977	5.288	8.265	0.825
100	1.285	3.151	1.086	3.603	3.684	3.684	7.287	0.728
107	1.281	3.150	1.311	1.433	3.274	3.298	6.573	0.656
114	1.270	3.151	1.312	1.542	2.992	3.159	6.151	0.614
119	1.287	3.173	1.040	1.116	2.668	2.803	5.910	0.590
126	1.283	3.131	1.235	1.329	2.997	2.777	5.774	0.577
136	1.274	3.127	1.149	1.260	2.543	2.367	4.910	0.490
146	1.276	3.159	1.309	1.356	2.187	1.967	4.154	0.415
160	1.270	3.140	1.140	1.262	1.776	1.641	3.418	0.341
175.5	1.261	3.139	1.536	1.548	1.542	1.375	2.917	0.291

[a] mms^{-1}. [b] Arbitrary units. [c] The subscripts refer to lower (–) and higher (+) velocity resonance lines respectively. [d] Normalized to 77 K.

TABLE 11

TIN-119 MÖSSBAUER DATA FOR $[ClEt_2SnOSnEt_2Cl]_2$

Temp. (K)	I.S. [a]	Q.S. [a]	Γ_- [a, c]	Γ_+ [a, c]	A_- [b, c]	A_+ [b, c]	Total resonance area [b]	Realtive % age effect [d]
77	1.496	3.410	1.359	1.311	14.645	13.366	29.011	1.000
81	1.497	3.410	1.543	1.437	14.016	13.337	27.850	0.961
86	1.502	3.411	1.268	1.230	12.951	12.702	26.646	0.884
88.5	1.498	3.404	1.495	1.515	12.651	12.095	25.210	0.869
92	1.500	3.387	1.371	1.337	12.162	11.917	24.079	0.830
92.5	1.497	3.405	1.320	1.257	12.058	11.622	23.673	0.816
97	1.499	3.381	1.382	1.343	10.634	10.468	21.497	0.741
100	1.498	3.392	1.250	1.205	10.365	10.135	20.888	0.720
103	1.494	3.383	1.291	1.245	8.222	8.082	16.623	0.573
110	1.499	3.372	1.302	1.227	6.228	6.093	12.562	0.433
111.5	1.496	3.384	1.125	1.073	5.506	5.455	11.169	0.385
119	1.495	3.350	1.217	1.153	3.446	3.384	6.963	0.240
128.5	1.490	3.357	1.059	1.110	2.610	2.688	5.396	0.186
138.5	1.484	3.338	1.038	0.974	2.205	2.201	4.497	0.155
145	1.469	3.314	1.127	1.045	1.848	1.897	3.800	0.131
154	1.482	3.337	1.044	0.970	1.493	1.454	2.988	0.102

[a] mms^{-1}. [b] Arbitrary units. [c] The subscripts refer to lower (—) and higher (+) velocity resonance lines respectively. [d] Normalised to 77 K.

TABLE 12

VARIATION OF I.S. AND Q.S. WITH R IN $[ClR_2SnOSnR_2Cl]_2$ COMPOUNDS [a]

R	I.S. [b]	Q.S. [b]
Me	1.28	3.17
Et [c]	1.50	3.41
n-Pr	1.45	3.26
n-Bu [c]	1.46	3.26
Ph	1.26	3.08

[a] Recorded at 77 K. [b] mms^{-1}. [c] These data agree well with those listed in ref. 19.

NMR spectrum [2]. On the basis of I.S. and Q.S. data alone, elucidation of the geometry and stereochemistry about the tin atom(s) is impossible, due to the high numbers of variable present. The magnitude of the Q.S. in each case indicates coordination-number of greater than four at the tin, but cannot satisfactorily distinguish between five- and six-coordination at the tin or a trigonal bipyramidal, octahedral or an intermediate geometry about the tin. The increase in the I.S. on going from the methyl- to the ethyl-derivative indicates a corresponding increase in the *s*-character of the tin—carbon bonds. Two factors, operating simultaneously, can account for this: (a) changes in orbital hybridisation resulting in an increased linearity of the $[C_2Sn]$ moiety in the ethyl-derivative. This is consistent with the observed opening of the C—Sn—C angle from 140.6(9)° or 135.3(7)°, (C(3)—Sn(1)—C(4) and C(1)—Sn(2)—C(2), respectively) in the methyl-derivative to 140(1), 157(6), 150(5) or 147(4)° (depending on the combination of disordered α-carbons at Sn(1) in the ethyl derivative; (b) the +I effect of the alkyl groups will also tend to increase electron density at the tin. The increase in I.S. on increase of alkyl chain length (Table 12) follows the expected pattern of +I strengths: Me < Et ~ n-Pr ~ n-Bu. Since the I.S. of the ethyl-, n-propyl and n-butyl derivatives are almost identical, assuming an equivalence of their respective +I effect values, it may be inferred that the C—Sn—C bond angle in these compounds is more or less constant. The —I effect of a phenyl group would be expected to reduce the I.S. value, so the similarity of I.S. values of the phenyl- and methyl-derivatives (1.26 mm s^{-1} and 1.28 mm s^{-1} respectively) must be due to an increase in the linearity of the $[C_2Sn]$ moiety in the presence of relatively bulky phenyl groups.

The strength of the Mössbauer resonance is dependent on the magnitude of the recoilless resonant interaction, which, in physical terms corresponds to the strength of the binding of the Mössbauer nucleus within the solid lattice. On a quantitative basis, the presence of a room temperature Mössbauer resonance is indicative of a polymeric lattice [20,21] although in a relatively recent publication by Bancroft et al. [22], exceptions to this rule have been demonstrated. The rate of decay of the resonance, is however, more conclusive. We have recently [23] shown that, for a series of organotin compounds, the rates of decay of polymeric and non-polymeric lattices are markedly different and that the slope (a) of the straight line obtained by plotting ln(relative % area) against temperature gives a reliable guide to the relative strength of the intermolecular interactions in the solid lattice.

In the "thin-absorber" approximation the resonance area (A) is related to the recoil-free fraction (f), which in turn is related to the mean-square amplitude of vibration of the tin atom $\langle x^2 \rangle$:

$$A = \frac{\pi}{2} f \Gamma \epsilon$$

$$f = \exp\left[\frac{-E_\gamma{}^2 \langle x^2 \rangle}{\hbar^2 c^2}\right]$$

where Γ is the half-height line width, ϵ an absorption term and E_γ is the energy of the Mössbauer transition. By equating these two expressions, it can be seen that the more persistent the peak area with increasing temperature, the less the increase in atomic displacement of the Mössbauer atom, hence the stronger the binding within the lattice.

It has become convenient, albeit rather naively, to treat the temperature dependence of Mössbauer resonance area/recoil-free fraction data in terms of the high-temperature limit of the Debye model of solids. In this approximation ln f is given by the expression:

$$\ln f = \frac{-6E_R T}{k\theta_m{}^2} = aT$$

where E_R = the recoil energy and θ_m, the Mössbauer temperature, is a characteristic of the solid. Semi-logarithmic plots of ln A against T for the two compounds are illustrated in Figs. 8 and 9, respectively. That for $[ClMe_2SnOSnMe_2Cl]_2$ is linear in the temperature range 77—175.5 K, with no discontinuities, suggesting that the temperature dependence of the recoil-free fraction for each of the two tin atoms is, like the I.S. and Q.S., very similar. The implication is

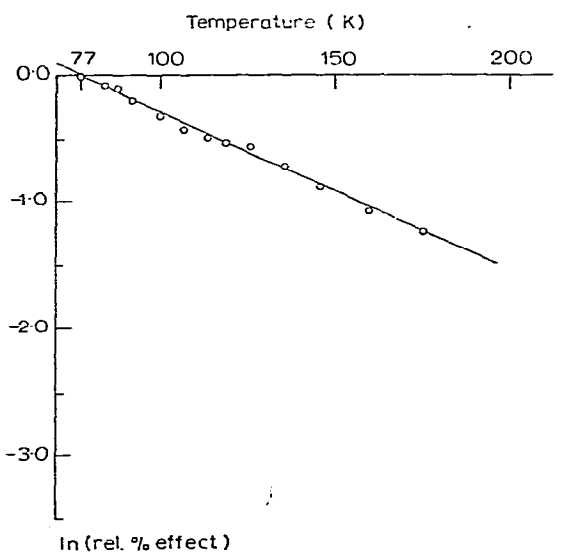

Fig. 8. Plot of ln(relative % effect) vs. temperature for $[ClMe_2SnOSnMe_2Cl]_2$.

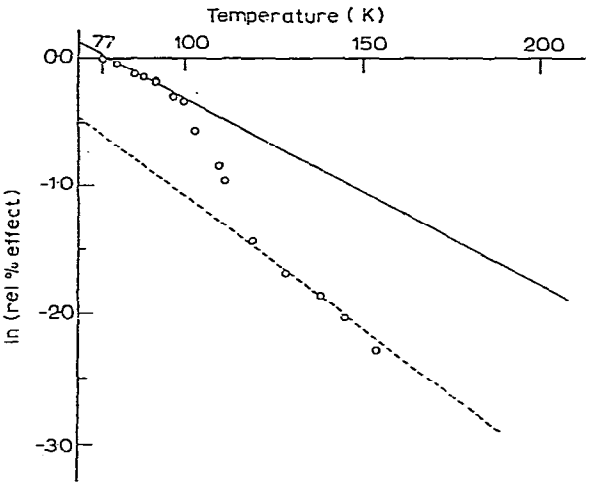

Fig. 9. Plot of ln(relative % effect) vs. temperature for $[ClEt_2SnOSnEt_2Cl]_2$.

that both are held in the crystal lattice similarly at low temperature as has been seen from the crystal structure determination at ambient temperatures.

Both tin atoms are bonded to two chlorines, two oxygens and two carbons in a geometric array midway between regular octahedral and trigonal bipyramidal geometry, and both have low principal anisotropic temperature factors, U_{11}, U_{22} and U_{33} (7.61(8), 6.05(7), 4.07(6) and 6.99(7), 6.93(7), 2.46(8) for Sn(1) and Sn(2) respectively (values $\times 10^2$)) indicating a low amplitude of thermal vibration in the solid state. The derived a-value of -1.26×10^{-2} K^{-1} lies between the value typical of a tightly bound polymeric lattice ($a = -0.8 \times 10^{-2}$ K^{-1}) and that typical of a non-interacting molecular solid (a -1.8×10^{-2} K^{-1}) [23]. The strength of the chlorine bridging observed in this compound is insufficient to confer an appreciable polymeric character on the lattice (hence the reduction in a-value from -1.8×10^{-2} to -1.26×10^{-2} K^{-1}) and is of similar strength to the hydrogen bonded lattice network seen in trimethyltin pyridylcarboxylate dihydrate (a -1.27×10^{-2} K^{-1}) [24].

The recoil energy, E_R, may be related to the effective recoiling mass containing the Mössbauer atom, M_{eff}, according to the conservation of momentum [25]:

$$E_R = \frac{E_\gamma^2}{2M_{eff}c^2}$$

and hence the slope of the ln A vs. T plot, a, is given by:

$$a = \frac{-3E_\gamma^2}{M_{eff}c^2k\theta_m^2}$$

An independent determination of θ_m will, therefore, yield an estimate of M_{eff}. Assuming that intramolecular forces are much stronger than the intermolecular forces and therefore do not couple (a gross assumption in the present case!) a value of $\theta_m(\equiv\theta_D)$ is available from the intra-unit cell intermolecular vibration

(ω_L) observed in the Raman spectrum, i.e.:

$$\theta_D = \frac{h\omega_L}{k}$$

and thus:

$$M_{eff} = \frac{-3E_\gamma{}^2 k}{ac^2h^2\omega_L{}^2}$$

The effect vibrating mass of 682 calculated from the band at 34.5 cm^{-1} in the Raman spectrum *, compares favourably with that expected of a [dimeric unit —2 Cl] (699). The lengthening of the Sn—Cl(2) bond (2.788(4) Å, Sn(1) and 2.710(5) Å, Sn(2), cf. Sn(1)—Cl(1): 2.438(4) Å) in order to facilitate both intra- and inter-molecular bridging effectively takes Cl(2) out of the primary coordination sphere of the tin nuclei so that it is now no longer part of the effective recoiling mass containing the Mössbauer atom.

Inspection of the ln A vs. T plot for $[ClEt_2SnOSnEt_2Cl]_2$ (Fig. 9) reveals two straight-line sections with a sharp discontinuity at ca. 110 K. No analogous behaviour has been observed previously for any other compounds, and no discontinuity is apparent in the I.S. data, but the Q.S. is reduced marginally above 111.5 K. In addition, the half-height linewidth, which at temperatures <110 K is rather high (mean 1.33 mms^{-1}, cf. $[ClMe_2SnOSnMe_2Cl]_2$ mean 1.27 mms^{-1}), but at temperatures in excess of 111.5 K decreases to a mean of 1.08 mms^{-1}, a value more characteristic of a single line rather than the resultant envelope of two overlapping resonances. The low-temperature region (77—100 K) of the plot is therefore attributed to the combined exponential decays of the recoil-free fraction of both tin nuclei, whilst the high temperature region (120—160 K) arises from the decay of the recoil-free fraction of only one of the tin nuclei; that of the other being negligible at these temperatures. The experimentally observed resultant recoil-free fraction decay may then be resolved into two components by assuming that the high temperature (120—160 K) straight-line (Fig. 10) is attributed to the recoil-free fraction decay of Sn(A) only. The equation of the best straight line through the points in the range 128.5—154 K is given by:

$$\text{Ln(relative \% effect)} = -0.02102T + 1.027$$

yielding a value of the relative % effect of Sn(A) at 77 K of 0.554. The relative % effect due to Sn(A) in the range 128.5—154 K can now be calculated relative to the value at 77 K, giving a best fit linear relationship of:

$$\text{ln(relative \% effect)} = -0.02074T + 1.597$$

from which it is possible to derive the relative % effect due to Sn(A) alone, normalised to 77 K, in the range 81—119 K, and hence by difference the corresponding values for Sn(B). The results are shown graphically in Fig. 10.

An assignment of Sn(A) and Sn(B) as Sn(1) and Sn(2), respectively, of the crystal structure determination would appear to be straight forward. Sn(A)

* Low frequency Raman bands at 22.5, 25(sh), 26, 26.5(sh), 33.5, 34.5, 40, 41, 42.5, 44, 47.5 and 56 cm^{-1}.

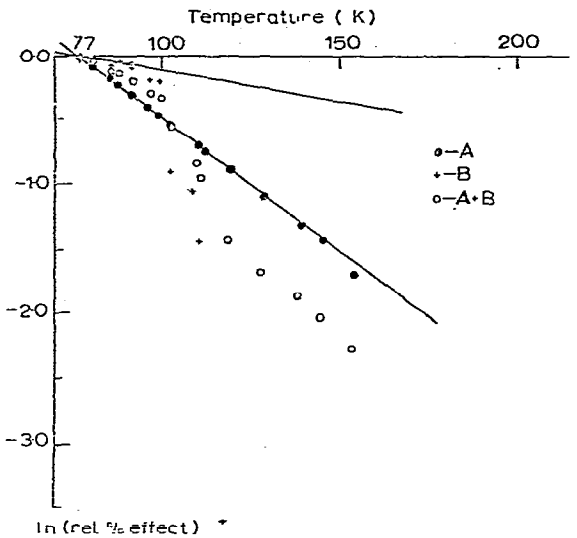

Fig. 10. Plot of ln(relative % effect) vs. temperature for $[ClEt_2SnOSnEt_2Cl]_2$ showing the resolution of the experimental into the contributions from each tin atom.

maintains a relatively intense resonance (hence recoil-free fraction) up to ca. 140 K, thus would be expected to have relatively little thermal motion and primary anisotropic temperature factors similar to those observed in the analogous methyl-distannoxane. On the other hand, Sn(B) has a recoil free fraction approaching 0 at ca. 110 K, and a corresponding increase in the respective anisotropic temperature factors would be expected. Examination of the final anisotropic thermal parameters derived from the X-ray structure determination of $[ClEt_2SnOSnEt_2Cl]_2$ (Table 7) shows that the values of the anisotropic thermal parameters U_{11}, U_{22} and U_{33} are between two and three times larger for Sn(2), (11.1(6), 13.0(6), 16.1(5) $\times 10^{-2}$) than the corresponding parameters for Sn(1), (5.0(2), 5.1(2), 6.3(2) $\times 10^{-2}$). Sn(A) can thus be correlated with Sn(1) and Sn(B) with Sn(2).

Thus, resolution of the experimentally obtained curve gives results which, at temperatures greater than ca. 110 K, give good correlation with the results of the X-ray diffraction study at room temperature. Below ca. 110 K, correlation with structural data obtained at room temperature is more difficult. The a-values for the two tins in the region 77—100 K are -2.07×10^{-2} K^{-1} (Sn(1)) and -0.49×10^{-2} K^{-1} (Sn(2)), and, although the errors in these values are obviously potentially quite large due to the assumption that the high temperature straight line in the experimentally derived plot is indeed linear over the whole 120—160 K range, the straight line for Sn(2) is more shallow than the corresponding line for Sn(1) i.e. Sn(2) is now more tightly bound than Sn(1). The data can thus be rationalised in two ways. Firstly, that the two tins are in similar lattice sites (like $[ClMe_2SnOSnMe_2Cl]_2$) and that the decrease in the recoil-free fraction at ca. 110 K is due to a phase change in the molecule as a whole. This would not, however, explain the differences in the values of the primary anisotropic thermal parameters at room temperature. Secondly, that resolution of

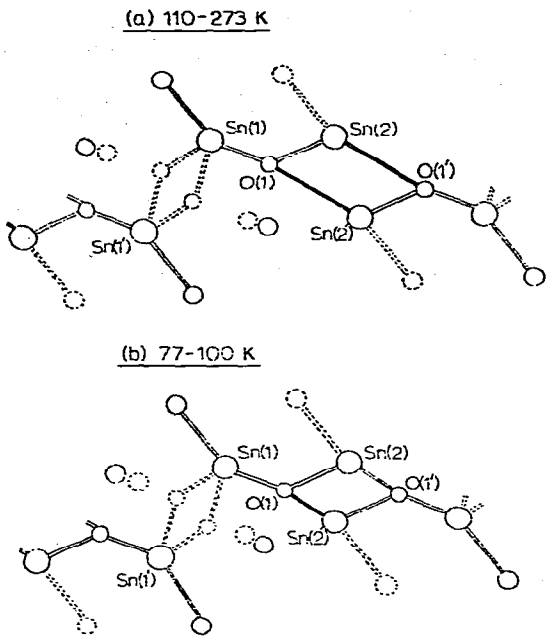

Fig. 11. Illustration of the proposed structural change occurring at Sn(2) at the transition temperature.

the data into the effects due to differing tins is essentially correct (within the outlined assumptions), and that a phase change occurs at ca. 110 K for Sn(2) only. Thus, the extent to which Sn(1) is bound within the lattice remains unchanged over the range 77 K—293 K, but below 100 K, Sn(2) is far more tightly bound than it is above 110 K.

If this interpretation of the data is correct, a possible phase change can be rationalised on the basis of the room temperature solid structure. As the temperature approaches 77 K, a damping of the amplitude of thermal vibration of the bridging oxygens and anionic chlorines will occur, so a contraction of the polymeric stannoxane ribbons takes place, stabilising primarily Sn(2) by (a) a shortening of the weak (3.48(20) Å) Sn—O linkage in Fig. 5(A) and (b) by a contraction of the Cl^-···Sn bridges retaining the particularly weakly bound Sn(2) (Fig. 5(B)) in the polymeric chain (Fig. 11).

This is the first reported instance of a change in lattice structure of an organotin compound at low temperatures, observed by Mössbauer spectroscopy.

The a-value of -1.46×10^{-2} K^{-1}, obtained from the initial straight line part of the experimentally determined ln(rel. % effect) v temperature (77—100 K) plot (Fig. 8) indicates a somewhat weaker polymeric lattice than was observed for the corresponding methyldistannoxane (a -1.26×10^{-2} K^{-1}). Provided that the ribbons of loosely bound dimeric units, known to exist in this compound at room temperature, remains essentially unaltered, consistency between the empirically suggested structure (variable temperature Mössbauer data) and known structure (X-ray crystallography) is maintained.

The effective vibrating mass of 894, calculated from the band at 28.0 cm^{-1}

in the Raman spectrum *, is in good agreement with the value for a dimeric mass of 882. The anionic chlorine atoms are now part of the effective recoiling mass containing the Mössbauer atom, unlike the corresponding atoms in the methyl analogue. The relative importance of the tin—chlorine involving the anionic chlorine in the two cases is presumed to be the dominating factor. In the methyl compound, Sn—Cl^- bridges link separate $[R_4Sn_2Cl_2O]_2$ units, but are essentially superfluous to the internal rigidity of the dimer. This is also true of the structure of the ethyl-distannoxane shown in Fig. 5(A), although the stannoxane ring is now much weaker (Sn(2)—O(1) 2.24(17) Å, Sn(2)—O(1) 3.48(20) Å) than in the methyl compound (Sn(2)—O(1) 2.054(8) Å, Sn(2)—O(1′) 2.115(9) Å). However, in the structure shown in Fig. 5(B), the Sn—Cl^- bridges not only coordinate differing $[R_4Sn_2Cl_2O]_2$ units, but are responsible for holding together individual $[R_4Sn_2Cl_2O]_2$ units via intramolecular bridging, hence maintaining them in the first coordination sphere of the tin nuclei.

Acknowledgement

We thank the S.R.C. for the award of a studentship (to K.C.M.).

References

1 P. Pfeiffer and O. Brach, Z. Anorg. Chem., 87 (1914) 229.
2 D.L. Alleston, A.G. Davies, M. Hancock and R.F.M. White, J. Chem. Soc., (1963) 5469.
3 R. Okawara, Proc. Chem. Soc., (1961) 383.
4 Y.M. Chow, Inorg. Chem., 10 (1971) 673.
5 Z.V. Zvonkova, Acta Cryst. A, 21 (1966) 155.
6 C.D. Garner, B. Hughes and T.J. King, Inorg. Nucl. Chem. Letters, 12 (1976) 859.
7 R. Graziani, G. Bombieri, E. Forsellini, P. Furlan, V. Peruzzo and G. Tagliavini, J. Organometal. Chem., 125 (1977) 43.
8 R. Fagliani, J.P. Johnson, I.D. Brown and R. Birchall, Acta Cryst. B, 34 (1978) 3743.
9 CRYSTALS program, Oxford University, Crystallography Computer Programs.
10 International Tables for X-ray Crystallography, Vol. III, Kynoch Press, Birmingham, 1962.
11 D.H. Johnson, E. Fritz, D.D. Halvorson and R.L. Evans, J. Amer. Chem. Soc., 77 (1955) 5857.
12 C.C. Addison, P.G. Harrison, N. Logan, L. Blackwell and D.H. Jones, J. Chem. Soc. Dalton, (1975) 1455.
13 N.T. Bokii, G.N. Zakharov and Yu.T. Struchkov, J. Struct. Chem., 11 (1970) 828.
14 P.G. Harrison, T.J. King and J.A. Richards, J. Chem. Soc. Dalton, (1976) 1414.
15 E.O. Schlemper, W.C. Hamilton, Inorg. Chem., 5 (1966) 995.
16 L.E. Sutton, International Distances, The Chemical Society, London, 1958.
17 A.G. Davies, H.J. Milledge, D.C. Puxley and P.J. Smith, J. Chem. Soc. (A), (1970) 2862.
18 N.W. Alcock and J.F. Sawyer, J. Chem. Soc. Dalton, (1977) 1090.
19 P.J. Smith, Organometal. Chem. Revs. (A), 5 (1970) 373.
20 G.M. Bancroft and R.H. Platt, Adv. Inorg. Radiochem., 15 (1972) 59.
21 J.F. Duncan and R.M. Golding, Quart. Revs., 19 (1965) 36.
22 G.M. Bancroft, K.D. Butler and T.K. Sham, J. Chem. Soc. Dalton, (1975) 1483.
23 P.G. Harrison, R.C. Phillips and E.W. Thornton, J. Chem. Soc. Chem. Commun., (1977) 603.
24 R.C. Phillips, Ph.D. Thesis, University of Nottingham, 1976.
25 R.H. Herber and Y. Hazony, J. Phys. C, 6 (1974) 131.
26 P.G. Harrison, K.C. Molloy and E.W. Thornton, Inorg. Chim. Acta, 33 (1978) 137.

* Low frequency Raman bands at 20, 21, 24, 28, 35, 37, 42, 46, 48, 53 and 56 cm^{-1}.